КОМПЬЮТЕРНЫЕ ТЕХНОЛОГИИ В ФИЗИКЕ

ON THE e/π IDENTIFICATION APPLYING THE CBM TRD: COMPARISON OF MEASUREMENTS WITH THE TRD PROTOTYPE AND GEANT3 SIMULATION AT $p = 1.5$ GeV/c

T. P. Akishina[a]*, O. Yu. Denisova*[a]*, V. V. Ivanov*[a]*, S. A. Lebedev*[a,b]

[a] Joint Institute for Nuclear Research, Dubna
[b] Gesellschaft für Schwerionenforschung mbH, GSI, Darmstadt, Germany

The comparison of the distributions of the e/π energy losses in the TRD prototype and GEANT3 simulation of the n-layered TRD realized in frames of the CBM ROOT at $p = 1.5$ GeV/c has shown that the GEANT3 simulation reproduces real data quite well. However, contrary to the real measurements, this does not permit one to obtain a comparable level of pions suppression for GEANT3 data using the most powerful method based on a likelihood functions ratio test. It is shown that the procedure of preparation of data sets corresponding to the n-layered TRD based on prototype measurements is a reason of reaching an erroneous and highly overestimated level of pions suppression. It is also demonstrated that the needed level of pions suppression could be achieved using a combined method, which is more simple for practical application.

Сравнение распределений потерь энергии e/π с импульсом 1,5 ГэВ/c в прототипе TRD и GEANT3-моделирование n-слойного детектора TRD, выполненные в среде CBM ROOT, показали, что результаты моделирования хорошо воспроизводят реальные данные. Однако, в отличие от реальных измерений, это не позволяет получить для данных GEANT3 сопоставимый уровень подавления пионов с помощью наиболее мощного метода на основе критерия отношения функций правдоподобия. Показано, что процедура подготовки наборов данных для n-слойного TRD на основе реальных измерений является причиной ошибочного, сильно завышенного уровня подавления пионов. Также показано, что необходимый уровень подавления пионов может быть достигнут с помощью комбинированного метода, который более прост для практических применений.

PACS: 29.40.Gs; 02.70.Rv; 02.50.Sk

INTRODUCTION

The CBM (Compressed Baryonic Matter) Collaboration [1,2] builds a dedicated heavy-ion experiment to investigate the properties of highly compressed baryon matter as it is produced in nucleus–nucleus collisions at the Facility for Antiproton and Ion Research (FAIR) in Darmstadt, Germany.

The experimental setup should comply with the following requirements: identification of electrons that requires a pions suppression factor of the order of 10^5, identification of hadrons with large acceptance, determination of the primary and secondary vertexes (accuracy $\sim 30\,\mu$m), high granularity of the detectors, fast detector response and read-out, very small

detector dead time, high-speed trigger and data acquisition, radiation hard detectors and electronics, tolerance towards delta-electrons.

Figure 1 shows a schematic view of the CBM experimental setup. Inside the dipole magnet gap, there are a target and planes of the Silicon Tracking System (STS) consisting of pixel and strip detectors. The Ring Imaging Cherenkov detector (RICH) has to detect electrons. The Transition Radiation Detector (TRD) measures electrons with momentum above 1 GeV/c. The time-of-flight detector consists of Resistive Plate Chambers (RPC). The Electromagnetic Calorimeter (ECAL) measures electrons, photons and muons.
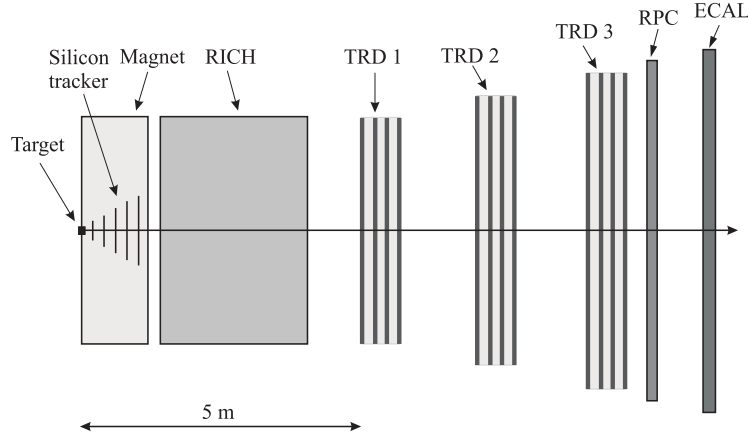
Fig. 1. Schematic view of the CBM experimental setup

The measurement of charmonium is one of the key goals of the CBM experiment. For detecting J/ψ meson in its dielectron decay channel, the main task is the separation of electrons and pions. The TRD must provide effective electron identification, sufficient pions suppression and tracking of all charged particles. The required pions suppression is a factor of about 100–200 and the required position resolution is of the order of 200–300 μm [2]. To fulfill these requirements, a careful optimization of the detector is needed.

In the technical proposal of the CBM experiment preliminary results were presented on the estimation of the electron identification and pions suppression applying a Likelihood Functions Ratio (LFR) test (see details in [2]). These studies have demonstrated that the TRD with 9 to 12 layers may fulfill the required electron/pion identification for the CBM experiment.

Here we analyze the efficiency of the electron/pion identification at $p = 1.5$ GeV/c based on real measurements of energy deposits in the TRD prototype and GEANT3 simulation of the n-layered TRD realized in frames of the CBM ROOT [3].

We show that the GEANT3 simulations quite well reproduce real measurements both for pions and electrons. However, contrary to real measurements, this does not permit one to obtain a comparable level of pions suppression for the LFR test. Based on the detailed analysis of GEANT3 data, we show that the procedure of preparing the data sets corresponding to the n-layered TRD based on real measurements is a reason of getting an erroneous, highly overestimated level of pions suppression. We also demonstrate that the needed level of pions suppression could be achieved using a combined method, which is more simple from a practical point of view.

1. DISTRIBUTIONS OF e/π ENERGY LOSSES IN THE TRD

Figure 2 shows a distribution of the measurements of ionization losses (dE/dx) for pions, and Fig. 3 gives energy losses for electrons (dE/dx and the Transition Radiation (TR)) in the TRD prototype with one layer: beam-test in GSI, $p = 1.5$ GeV/c, February 2006.
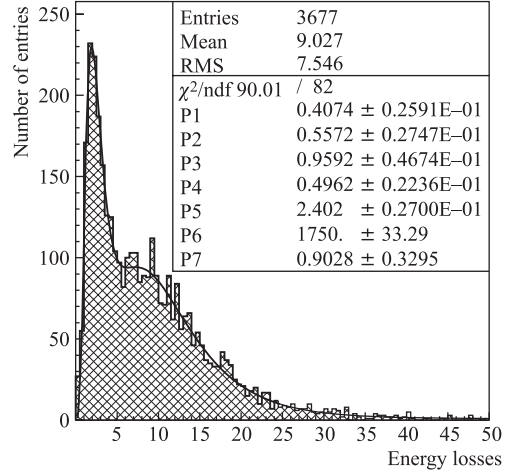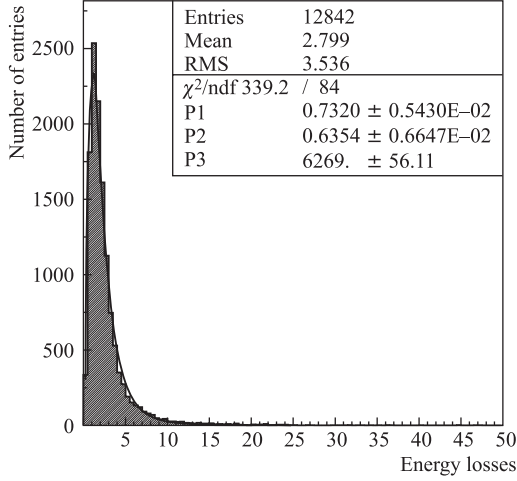
Fig. 2. Distribution of pion energy losses in the TRD prototype and its approximation by log-normal function (1)

Fig. 3. Distribution of electron energy losses in the TRD prototype and its approximation by a weighted sum of two log-normal functions (2)

The distribution of the pion ionization losses in the TRD prototype (Fig. 2) is quite well approximated by a log-normal function [4]

$$f_1(x) = \frac{A}{\sqrt{2\pi}\sigma x} \exp\left[- \frac{1}{2\sigma^2}(\ln x - \mu)^2 \right], \tag{1}$$

where σ is a dispersion; μ is a mean value, and A is a normalizing factor [5]. The correspondences between the parameters of formula (1) and Fig. 2 are as follows: $\sigma =$ P1, $\mu =$ P2, and $A =$ P3.

The distribution of energy losses of electrons (dE/dx and TR) is approximated with a high accuracy by a weighted sum of two log-normal distributions [4] (see Fig. 3),

$$f_2(x) = B\left(\frac{a}{\sqrt{2\pi}\sigma_1 x} \exp-\left[\frac{1}{2\sigma_1^2}(\ln x - \mu_1)^2\right] + \frac{b}{\sqrt{2\pi}\sigma_2 x} \exp-\left[\frac{1}{2\sigma_2^2}(\ln x - \mu_2)^2\right] \right) + c, \tag{2}$$

where σ_1 and σ_2 are dispersions; μ_1 and μ_2 are mean values; a and $b = 1 - a$ are the contributions of the first and second log-normal distributions, correspondingly; c is a shift parameter, and B is a normalizing factor. The correspondences between the parameters of

formula (2) and Fig. 3 are as follows: $a = P1$, $\sigma_1 = P2$, $\mu_1 = P3$, $\sigma_2 = P4$, $\mu_2 = P5$, $B = P6$, and $c = P7$.

A second set of data included GEANT3 simulations for pions and electrons with momentum $p = 1.5$ GeV/c, and satisfied the following selection criteria: 1) they should be emitted from the primary vertex, and 2) must have momenta larger 0.5 GeV/c at the entrance to the first TRD station.

Figure 4 shows a distribution of energy losses of pions, and Fig. 5 presents a distribution of energy losses of electrons in one layer of the TRD for the GEANT3 simulation. We see that the pions distribution is quite well approximated by a log-normal function (1), and the electrons distribution — by a weighted sum of two log-normal functions (2): see Figs. 4 and 5.
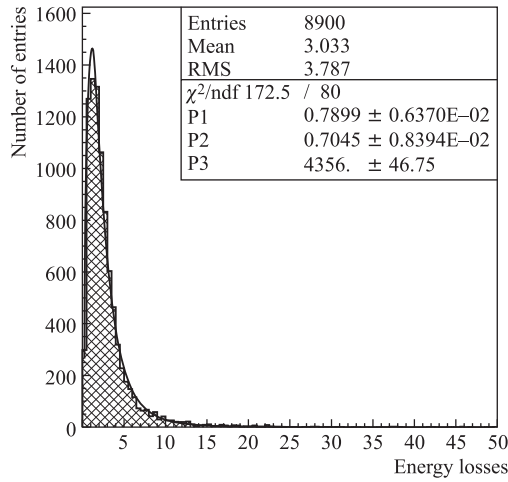
Fig. 4. Distribution of pion energy losses in one layer of the TRD and its approximation by log-normal function (1): GEANT3 simulation
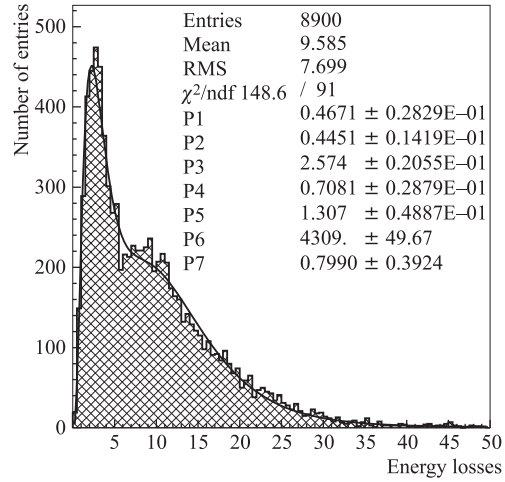
Fig. 5. Distribution of electron energy losses in one layer of the TRD and its approximation by a weighted sum of two log-normal functions (2): GEANT3 simulation

One can clearly see that the GEANT3 simulation of energy losses for pions (Fig. 4) and electrons (Fig. 5) well reproduces the real measurements: compare with Figs. 2 and 3. The results of this comparison are presented in Table 1.

Table 1. **Comparison of the mean value (m.v.) and RMS of the energy deposit distributions for real measurements and GEANT3 simulation**

Type of data	m.v. (π)	RMS (π)	m.v. (e)	RMS (e)
TRD prototype	2.799	3.536	9.027	7.546
GEANT3	3.033	3.787	9.585	7.699

These results of the GEANT3 simulation significantly differ from those presented in [4]. The main reason of such a difference consists in that the GEANT3 simulation data in [4] contained an admixture ($\sim$ 15–16%) of events which did not have the TR deposits in any of TRD layers: the corresponding details will be discussed in Sec. 3.

2. EFFICIENCY OF THE e/π IDENTIFICATION FOR REAL MEASUREMENTS AND GEANT SIMULATION

The particle identification problem (in our case, pions and electrons) using n-layered TRD consists in the following: having a set of n measurements of energy losses from n layers of the TRD, one should determine to what distribution (pion or electron) the energy losses of the particle registered by the TRD are relative.

For real measurements, only measurements and distributions of the energy deposits in a single-layer TRD prototype are available. To prepare a set of n «measurements» of energy losses corresponding to a particle (electron or pion) passing through the n-layered TRD, we used a subroutine HISRAN [6] that allows one to generate n random values in accordance with a given distribution. The distributions related to pions and electrons are supplied in the form of histograms presented in Figs. 2 and 3 using a subroutine HISPRE [6] (once for each histogram).

A uniform random number is generated using RNDM [7]. This number is then transformed to a user's distribution using a cumulative probability distribution constructed from the user's histogram. The cumulative distribution is inverted by using a binary search for the nearest bin boundary and a linear interpolation within the bin.

To estimate the efficiency of particle identification, we used three approaches:
• LFR test,
• ω_n^k goodness-of-fit criterion [8, 9],
• a combined method (see [10]), which includes a successive application of two statistical criteria: 1) the mean value method, and 2) the ω_n^k test.

2.1. Efficiency of the e/π Identification Using the LFR Test. The LFR test (see, for example, [5, 8]) could be related to Neiman–Pirson criterion which is the most powerful criterion for testing the hypothesis H_0 (in our case, the distribution of electrons) against the alternative hypothesis H_1 (the distribution of pions) [5]. Therefore, for the given significance level α the value of β could be considered as a minimally possible one. In our case, this corresponds to the maximumal factor of the pions suppression.

While applying the likelihood test to our problem, the value [11, 12]

$$L = \frac{P_e}{P_e + P_\pi}, \qquad P_e = \prod_{i=1}^{n} p_e(\Delta E_i), \qquad P_\pi = \prod_{i=1}^{n} p_\pi(\Delta E_i), \qquad (3)$$

is calculated for each event, where $p_\pi(\Delta E_i)$ is the value of the density function p_π in the case when the pion loses energy ΔE_i in the ith absorber, and $p_e(\Delta E_i)$ is a similar value for electron.

To calculate the values of density functions $p_\pi(\Delta E_i)$ and $p_e(\Delta E_i)$ the approximations of distributions of energy losses for pions and electrons by functions (1) and (2) were used.

Figure 6 shows the distributions of the variable L for the data set generated on the basis of real measurements in accordance with the procedure described above: when only pions (Fig. a) or electrons (Fig. b) pass through the n-layered TRD.
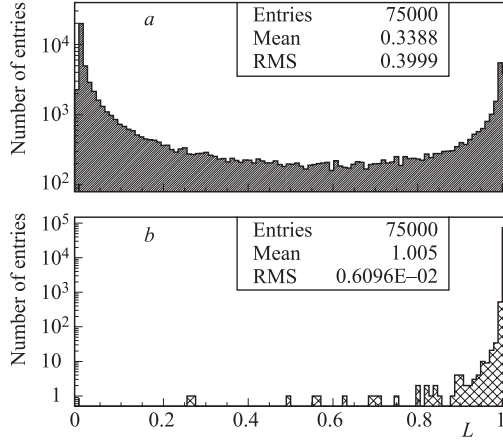
Fig. 6. TRD prototype: distributions of L for pions (a) and electrons (b) pass through the TRD with $n = 12$ layers
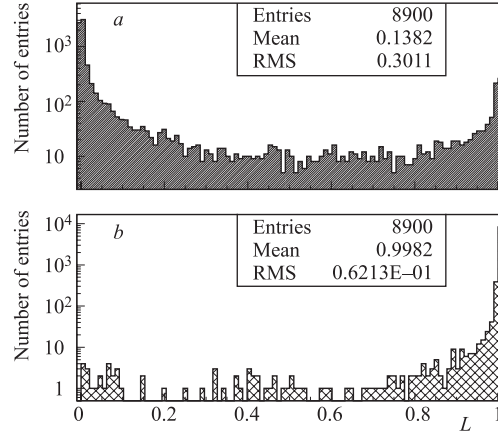
Fig. 7. GEANT3 simulation: distributions of L for pions (a) and electrons (b) pass through the TRD with $n = 12$ layers

The efficiency of registered electrons is determined by the ratio of the electrons selected in the admissible region for the pre-assigned significance level α (first-order error) to part β of pions having hit in the admissible region (second-order error).

In our case α value was set equal to 10%. This means that in the admissable region there must remain 90% of electrons. For this value of α the second-order error β constituted 0.925%. Thus, the suppression factor of pions that is equal to $100/\beta$, makes up 108.

It must be noted here that this factor of the pions suppression significantly differs from a similar value presented in [4]. The reason consists in the fact that when in [4] the values of the density functions corresponding to electrons p_e and pions p_π in Eq. (3) were calculated, one used the parameters obtained as a result of fitting the distributions of energy losses, including the normalizing factors P3 for pions and P6 for electrons: see Figs. 2 and 3. These two parameters depend on a statistics volume in the histogram, which greatly differs for pions (12842 entries) and electrons (3677 entries).

In order to exclude this dependence on the statistics volume, we equated the parameters P3 and P6, which are equivalent to the identical number of entries in the histograms for electrons and pions at the distributions fitting stage.

The distributions of the variable L for the data set based on GEANT3 simulation are presented in Fig. 7. In this case for $\alpha = 10\%$ the corresponding second-order error $\beta = 2.416\%$. Thus, the pions suppression factor constitutes 41, which is significantly smaller than 108.

2.2. Efficiency of the e/π Identification Using the ω_n^k Test. This test is based on a comparison of the distribution function $F(x)$ corresponding to a pre-assigned hypothesis

(H_0) with the empirical distribution function $S_n(x)$ [13,14]:

$$S_n(x) = \begin{cases} 0, & \text{if} \quad x < x_1; \\ i/n, & \text{if} \quad x_i \leqslant x \leqslant x_{i+1}, \quad i = 1, \ldots, n-1, \\ 1, & \text{if} \quad x_n \leqslant x. \end{cases} \tag{4}$$

Here $x_1 \leqslant x_2 \leqslant \ldots \leqslant x_n$ is the ordered sample (*variational series*) of size n constructed on the basis of observations of variable x.

The testing statistics is a measure of «distance» between $F(x)$ and $S_n(x)$. Such statistics are known as *non-parametric*. We suggested and investigated a new class of non-parametric statistics [13]

$$\omega_n^k = -\frac{n^{k/2}}{k+1} \sum_{i=1}^{n} \left\{ \left[\frac{i-1}{n} - F(x_i) \right]^{k+1} - \left[\frac{i}{n} - F(x_i) \right]^{k+1} \right\}. \tag{5}$$

The goodness-of-fit criteria constructed on the basis of these statistics are usually applied for testing the correspondence of each sample to the distribution known *a priori*.

On the basis of the ω_n^k test, a method has been developed for analysis of rare multidimensional events [8,14,15]:

1. The sample to be analyzed is transformed («normalized») so that the contribution of a dominant distribution is described by the distribution function $F_b(x)$.

2. Each sample composed of the values pertaining to the transformed distribution, is tested with the ω_n^k goodness-of-fit criterion for correspondence to the $F_b(x)$ hypothesis. In this process, the abnormal events which do not comply with H_0 correspond to the large absolute values of the ω_n^k-statistic, resulting in their clustering in the critical region.

The energy losses of pions have a form of Landau distribution [16]. We use it as H_0 to transform the initial measurements to a set of variable λ:

$$\lambda_i = \frac{\Delta E_i - \Delta E_{\text{mp}}^i}{\xi_i} - 0.225, \qquad i = 1, 2, \ldots, n, \tag{6}$$

ΔE_i — energy loss in the ith absorber; ΔE_{mp}^i — the value of the most probable energy loss, $\xi_i = \dfrac{1}{4.02}$ FWHM of distribution of pions energy losses [8].

In order to determine the value of the most probable energy loss ΔE_{mp}^i and the value FWHM of the distribution of pions energy losses in the ith absorber, the indicated distribution was approximated by the density function of a log-normal distribution (Figs. 2 and 4).

The obtained λ_i, $i = 1, \ldots, n$ are ordered due to their values (λ_j, $j = 1, \ldots, n$) and used for calculation of ω_{12}^{10} (see (5), where $F(x) = \phi(\lambda)$). Here the values of Landau distribution function $\phi(\lambda)$ are calculated using the DSTLAN function (from the CERNLIB library [17]).

Figure 8 shows the distributions of ω_{12}^{10} values calculated for the prototype samples for pions (Fig. *a*) and electrons (Fig. *b*). The value of the second-order error β corresponding to the significant level $\alpha = 10\%$ of the ω_{12}^{10} test forms 1.152%. Thus, the pions suppression factor constitutes 87.

Figure 9 shows the distributions of ω_{12}^{10} values calculated for GEANT3 samples. For these data sets β forms 1.831%. This means that the pions suppression factor constitutes 55.
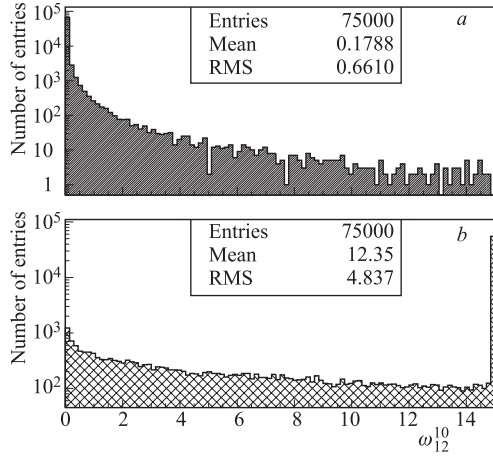
Fig. 8. TRD prototype: distributions of ω_{12}^{10} values calculated for pions (a) and electrons (b)
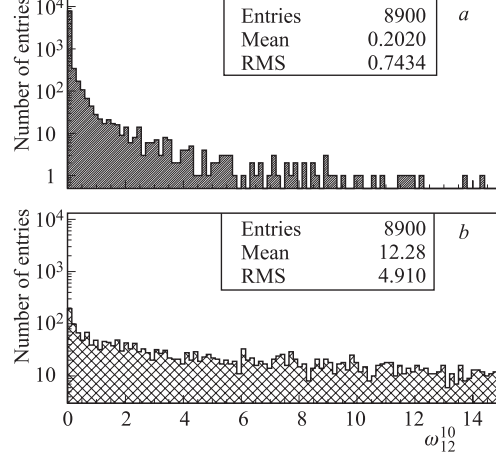
Fig. 9. GEANT3 simulation: distributions of ω_{12}^{10} values calculated for pions (a) and electrons (b)

2.3. Efficiency of the e/π Identification Using the Combined Method. The combined method is based on a successive application of two statistical criteria [10]: 1) the mean value method, and 2) the ω_{12}^{10} test.

In the mean value method (MVM) a variable value is calculated:

$$\overline{\Delta E} = \frac{1}{n} \sum_{i=1}^{n} \Delta E_i, \tag{7}$$

where n is the number of layers in TRD.

Figure 10 shows the distributions of the averaged energy losses $\overline{\Delta E}$ in the TRD prototype for pions (Fig. a) and electrons (Fig. b).

It is clearly seen that the distribution corresponding to pions is quite well separated from the electrons distribution. If we set the critical value $\overline{\Delta E}_{\mathrm{cr}} = 6.1$, then 92.33% of electrons will remain in the admissible region, and the second-order error will form 1.365%. Thus, the factor of pions suppression will constitute 73.

This result could be significantly improved, if we apply the ω_n^k test to the events selected in the admissible region. Figure 11 shows the corresponding distributions of ω_{12}^{10} for pions (Fig. a) and electrons (Fig. b). The critical value $\omega(k,n)_{\mathrm{cr}} = 0.7785$ permits us to save 90% of electrons in the admissible region, and the second-order error will form 0.128%. Thus, the pions suppression factor will constitute 781.

Figure 12 shows the distributions of variable $\overline{\Delta E}$ for GEANT3 simulation.

If we set the critical value $\overline{\Delta E}_{\mathrm{cr}} = 6.25$, then there will remain 92.38% of electrons in the admissible region, and the second-order error will form 6.517%. Thus, the factor of pions suppression will constitute 15.3.

We apply the ω_n^k test to the events selected in the admissible region. Figure 13 shows the corresponding distributions of ω_{12}^{10} for pions (Fig. a) and electrons (Fig. b). The critical value $\omega(k,n)_{\mathrm{cr}} = 0.7445$ permits one to save 90% of electrons in the admissible region,
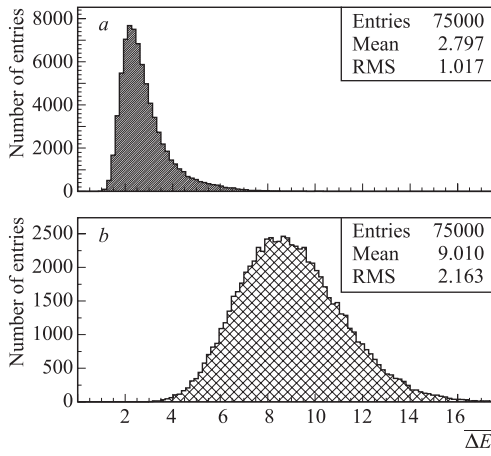
Fig. 10. TRD prototype: distribution of the averaged energy losses $\overline{\Delta E}$ for pions (*a*) and electrons (*b*)
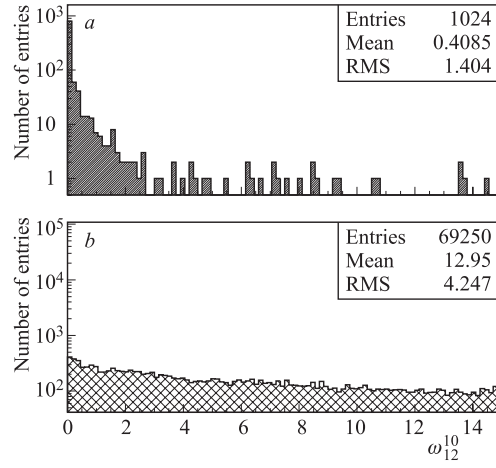
Fig. 11. TRD prototype: distribution of ω_{12}^{10} for events selected in the admissible region: for pions (*a*) and electrons (*b*)
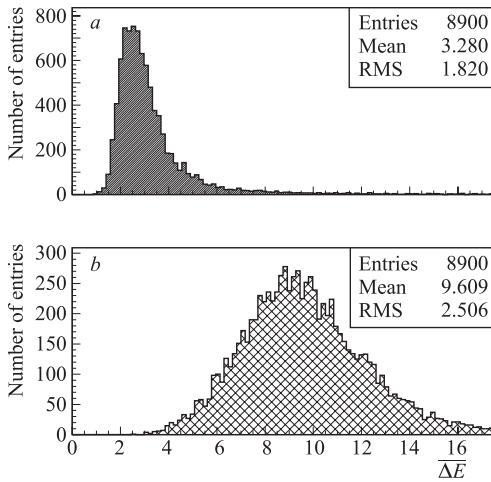
Fig. 12. GEANT3 simulation: distributions of variable $\overline{\Delta E}$ for pions (*a*) and electrons (*b*)
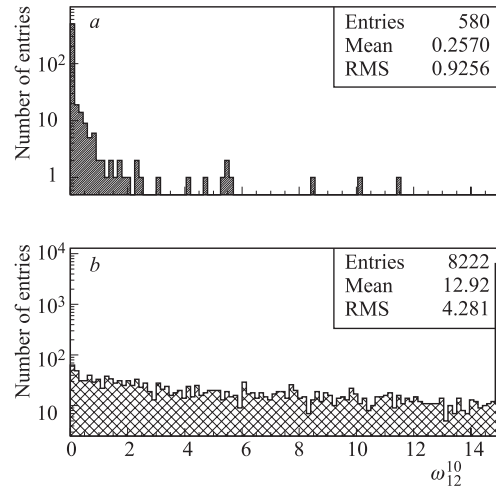
Fig. 13. GEANT3 simulation: distributions of ω_{12}^{10} for events selected in the admissible region: for pions (*a*) and electrons (*b*)

and the second-order error will form 0.382%. Thus, the factor of pions suppression will constitute 262. This value is significantly smaller as compared to the value obtained for the prototype data.

2.4. Discussion of the Obtained Results. The pions suppression factors corresponding to the 90% efficiency of electrons registration applying different methods are presented in Table 2.

Table 2. **The pions suppression factors for the 90% efficiency of electrons registration applying different methods**

Type of data	LFR	ω_{12}^{10}	MVM	MVM + ω_{12}^{10}
TRD prototype	108	83	73	781
GEANT3	41	55	17	262

This table demonstrates that the pions suppression factor obtained for the prototype measurements compared to those obtained for GEANT data:

1) differs for the LFR test approximately in 3 times,

2) has roughly the same level for the ω_{12}^{10} criterion,

3) differs for the MVM more than in 4 times,

4) for the combined (MVM+ω_{12}^{10}) method the difference is around 3 times.

Let us try to understand the reasons of such a difference and to reproduce (or not) the results obtained for the TRD prototype measurements.

3. THE ELECTRON ENERGY DEPOSITS IN THE TRD

As a first step, let us consider a process of forming the electron energy losses in the TRD. These losses are formed by the energy losses on the ionization and the transition radiation.

Figure 14 shows a distribution of the electron energy losses on the ionization, and Fig. 15 presents a distribution of the electron energy losses on the transition radiation in a single TRD layer.

Entries	8900
Mean	4.488
RMS	4.148
χ^2/ndf 173.7 / 80	
P1	0.6738 ± 0.6482E–02
P2	1.228 ± 0.7265E–02
P3	4343. ± 46.62
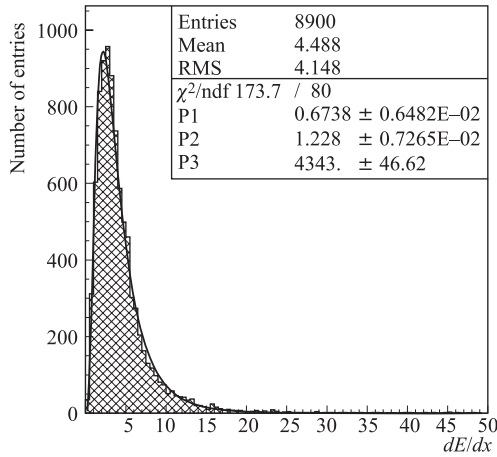
Fig. 14. GEANT3 simulation: distribution of electron energy losses on the ionization and its approximation by log-normal function (1)

Entries	8900
Mean	5.284
RMS	6.582
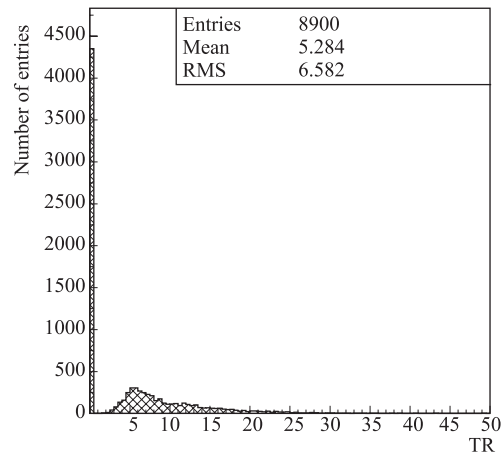
Fig. 15. GEANT3 simulation: distribution of electron energy losses on the transition radiation

Figure 16 shows a probability of events with a different number of TR counts. This distribution clearly shows that the most probable value of TR counts in the TRD with 12 layers is 6, and we almost do not have the events with TR counts in all 12 layers.

Entries	8900
Mean	6.023
RMS	1.892
χ^2/ndf 57.37 / 10	
Constant	1887. ± 24.64
Mean	6.024 ± 0.2049E–01
Sigma	1.870 ± 0.1406E–01
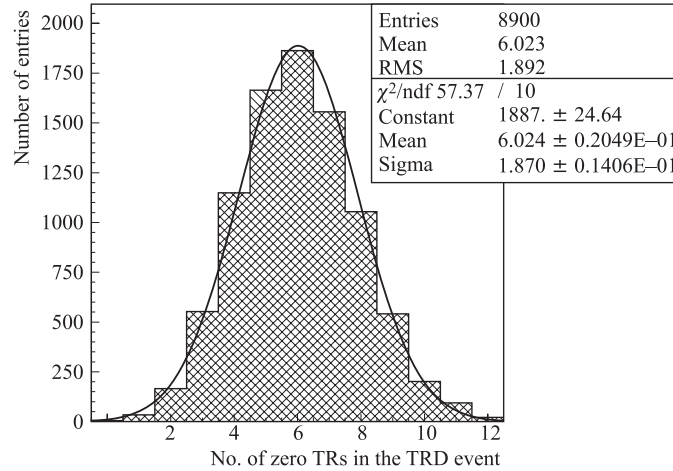
Fig. 16. GEANT3 simulation: distributions of events with different number of TR counts and its approximation by Gaussian distribution

It must be noted that when the electron passes the ith layer with TR = 0, then its energy loss follows the distribution of dE/dx losses (Fig. 14). By contrast, when we have the TR count in the ith layer, the electron energy loss will correspond to the sum of two distributions: dE/dx+TR (right distribution in Fig. 15).

Thus, the distribution of electron energy losses (in the case of GEANT3 simulation, and what we will have in the real experiment) is described by a complex hypothesis — the sum of 2 distributions. This means that its approximation by a weighed sum of two log-normal distributions (fitting curve in Fig. 5) may not give us a maximal value of pions suppression, if we use the LFR test, as in this test both hypotheses — the null-hypothesis and the alternative hypothesis — must be simple.

The difference for the prototype measurements and the GEANT3 simulation lies in the fact that in case of real data the energy losses in $n = 12$ layers of the TRD detector are generated in accordance with the distributions of energy losses for electrons and pions obtained in a single layer TRD prototype. Thus, for electrons these losses are described by one distribution (Fig. 3), i.e., by a simple hypothesis.

By analogy with the TRD prototype, let us generate the energy losses of electrons and pions in n layers of the TRD using the distributions obtained from the GEANT3 simulation in the single TRD layer and presented in Figs. 4 and 5.

The result of processing the data sets prepared in such a way with the help of the LFR test is presented in Fig. 17.

In this case, for α equal to 10%, the corresponding second-order error $\beta = 0.873\%$. Thus, the suppression factor of pions constitutes 114, which is very close to the value obtained for the prototype case.
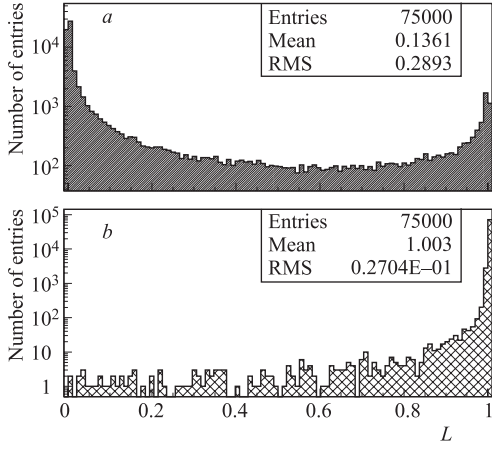
Fig. 17. GEANT3 histogram: distributions of L for pions (a) and electrons (b)
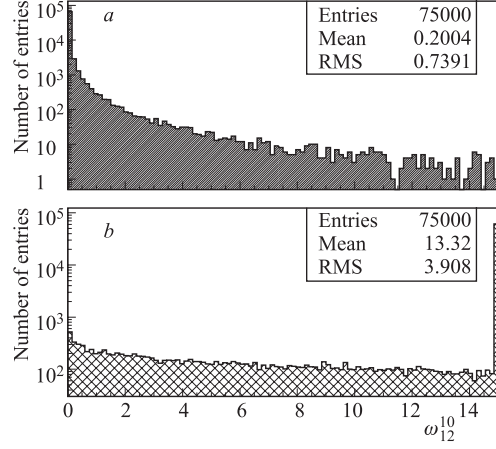
Fig. 18. GEANT3 histogram: distributions of ω_{12}^{10} values calculated for pions (a) and electrons (b)
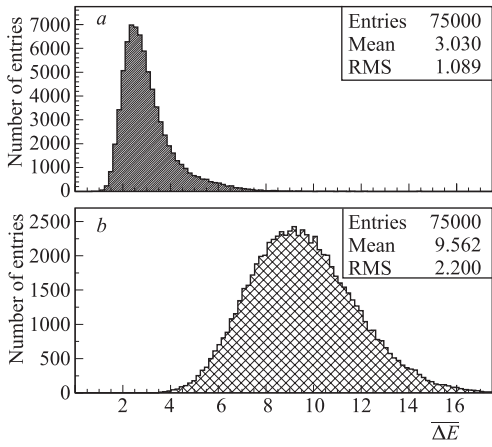
Fig. 19. GEANT3 histogram: distributions of variable $\overline{\Delta E}$ for pions (a) and electrons (b)
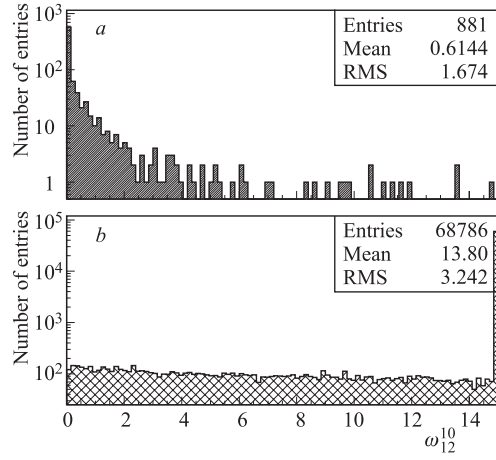
Fig. 20. GEANT3 histogram: distributions of ω_{12}^{10} for events selected in the admissible region: for pions (a) and electrons (b)

The result obtained for these data using the ω_{12}^{10} criterion is shown in Fig. 18. For the significant level $\alpha = 10\%$, the second-order error β will form 0.621%. Thus, the pions suppression factor will constitute 161, which is compatible with the value obtained for the prototype data.

Figure 19 shows the distributions of the averaged energy losses $\overline{\Delta E}$ for these data sets. If we set the critical value $\overline{\Delta E}_{\mathrm{cr}} = 6.65$, then 91.71% of electrons will remain in the admissible

region, and the second-order error will form 1.175%. Thus, the factor of pions suppression constitutes 85.

We apply the ω_n^k test to the events selected in the admissible region. Figure 20 shows the corresponding distributions of ω_{12}^{10} for pions (Fig. *a*) and electrons (Fig. *b*).

The critical value $\omega(k, n)_{\mathrm{cr}} = 1.485$ permits one to save 90% of electrons in the admissible region, and the second-order error will form 0.139%. Thus, the factor of pions suppression constitutes 721. This value is very close to the value obtained for the prototype data.

CONCLUSION

The comparison of the distributions of energy losses of pions and electrons with momentum $p = 1.5$ GeV/c in the single-layer TRD prototype, and with the help of the GEANT3 simulation of the n-layered TRD realized in frames of the CBM ROOT has shown that the indicated distributions are close to each other: see Table 1.

By using the mentioned data sets and three different statistical methods (LFR test, ω_n^k criterion, and combined MVM+ω_n^k method), we have studied the efficiency of the pion and electron identification with the help of the n-layered TRD: see Sec. 2.

Our analysis has shown that despite quite good coincidence of real measurements with the GEANT3 simulation, contrary to real measurements, we failed to obtain a comparable level of pions suppression for the most powerful method based on the LFR test. We have obtained a compatible results for ω_{12}^{10} criterion and a considerable divergence for the combined method: see Table 2.

In Sec. 3 we investigated the process of forming the energy losses by electrons in the TRD detector realized in frames of the CBM ROOT, and which is adequate to that available in the real experiment. This analysis has demonstrated that in approximately 1/2 cases we do not have TR counts in the TRD layers and that the most probable value of TR counts in the TRD with 12 layers is 6, and we almost do not have events with TR counts in all 12 layers.

This means that the distribution of the electron energy losses (the GEANT simulation) is described by a complex hypothesis — a sum of 2 distributions. As a result, its approximation by a single distribution, namely, a weighed sum of two log-normal distributions, may not give us a maximal value of the pions suppression, if using the LFR test.

Therefore, we have answered our first question, i.e., the difference in the results of the LFR test for real measurements and GEANT3 simulations.

The difference of data sets based on real measurements and GEANT3 simulation is that in the case of real data the energy losses for the $n = 12$ layers of the TRD detector were generated in accordance with the distribution of the energy losses of pions and electrons measured in the single-layer TRD prototype, i.e., for electrons those losses were described by a simple hypothesis.

In Sec. 3, by analogy with the TRD prototype, we generated the energy losses of electrons and pions in n layers of the TRD using the distributions (histograms) obtained from the GEANT3 simulations in a single TRD layer. The results of processing the obtained data sets are presented in Table 3.

Thus, on the one hand, we reproduced the results obtained on the basis of real measurements, and, on the other hand, we understood that we have to be oriented on the values presented in Table 2 for the line «GEANT3», because the procedure of preparation of data

Table 3. **The pions suppression factors for the 90% efficiency of electrons registration applying different methods**

Type of data	LFR	ω_{12}^{10}	MVM	MVM $+\omega_{12}^{10}$
TRD prototype	108	83	73	781
GEANT3 (histograms)	114	161	85	721

sets based on the real measurements is a reason of getting erroneous and highly overestimated pions suppression factor.

We also have demonstrated that the needed level of pions suppression could be achieved using a combined method (see Table 2), which is more simple from a practical viewpoint, because for its application only two parameters (see formula (6)) corresponding to the distribution of pions energy losses are needed.

REFERENCES

1. Letter of Intent for the Compressed Baryonic Matter Experiment. http://www.gsi.de/documents/DOC-2004-Jan-116-2.pdf

2. Compressed Baryonic Matter Experiment. Technical Status Report, GSI, Darmstadt, 2005. http://www.gsi.de/onTEAM/dokumente/public/DOC-2005-Feb-447 e.html

3. *Bertini D. et al.* The FAIR Simulation and Analysis Framework // Proc. of Intern. Conf. on Computing in High Energy and Nuclear Physics (CHEP'07), Victoria, BC Canada, 2007; J. Phys. Conf. Ser. http://www.gsi.de/fair/experiments/CBM

4. *Akishina E. P. et al.* Distributions of Energy Losses for Electrons and Pions in the CBM TRD. JINR Commun. E10-2007-158. Dubna, 2007. 15 p.

5. *Eadie W. T. et al.* Statistical Methods in Experimental Physics. Amsterdam; London: North-Holland Publ. Comp., 1971.

6. *James F.* CERN Computer Centre Program Library. V. 150.

7. *Eicken H., Lindelof T.* CERN Computer Centre Program Library. V. 104.

8. *Zrelov P. V., Ivanov V. V.* The Relativistic Charged Particles Identification Method Based on the Goodness-of-Fit ω_n^3-Criterion // Nucl. Instr. Meth. A. 1991. V. 310. P. 623–630.

9. *Akishina E. P. et al.* Electron/Pion Identification in the CBM TRD Applying a ω_n^k Goodness-of-Fit Criterion // Part. Nucl., Lett. 2008. V. 5, No. 2(144). P. 202–218.

10. *Akishina E. P. et al.* Comparative Analysis of Statistical Criteria for e/π Identification Using TRD in the CBM Experiment // Proc. of the XXI Intern. Symp. on Nuclear Electronics & Computing, Varna, Bulgaria, Sept. 10–17, 2007. Dubna, 2007.

11. *Andronic A. et al.* // Nucl. Instr. Meth. A. 2004. V. 519. P. 508.

12. *Ramaha Murty P. V., Demeester G. D.* // Nucl. Instr. Meth. 1967. V. 56. P. 93.

13. *Ivanov V. V., Zrelov P. V.* Nonparametric Integral Statistics $\omega_n^k = n^{k/2} \int\limits_{-\infty}^{\infty} [S_n(x) - F(x)]^k dF(x)$:

    Main Properties and Applications // Intern. J. Comp. & Math. Appl. 1997. V. 34, No. 7/8. P. 703–726; JINR Commun. P10-92-461. Dubna, 1992 (in Russian).

14. *Zrelov P. V., Ivanov V. V.* The Small Probability Events Separation Method Based on the Smirnov–Gramer–Mises Goodness-of-Fit Criterion. Algorithms and Programs for Solution of Some Problems in Physics. V. 6; Preprint KFKI-1989-62/M. Budapest, 1989. P. 127–142.

15. *Zrelov P. V. et al.* Simulation of Experiment on the Investigation of the Processes of the Subthreshold K^+ Production. JINR Preprint P10-92-369. Dubna, 1992; Math. Modeling. 1993. V. 4, No. 11. P. 56–74 (in Russian).

16. *Kolbig K. S., Schorr B.* // Comp. Phys. Commun. 1984. V. 31. P. 97.

17. *Koelberg K. S.* CERN Computer Centre Program Library. G. V. 110.